Hadron production in $p + p$, $p + \text{Pb}$, and $\text{Pb} + \text{Pb}$ collisions with the HIJING 2.0 model at energies available at the CERN Large Hadron Collider

Wei-Tian Deng,[1,2] Xin-Nian Wang,[3,4] and Rong Xu[3]

[1]*Frankfurt Institute for Advanced Studies (FIAS), Ruth-Moufang-Strasse 1, D-60438 Frankfurt am Main, Germany*
[2]*Department of Physics, Shandong University, Jinan 250100, People's Republic of China*
[3]*Institute of Particle Physics, Huazhong Normal University, Wuhan 430079, People's Republic of China*
[4]*Nuclear Science Division, MS 70R0319, Lawrence Berkeley National Laboratory, Berkeley, California 94720, USA*

The Heavy-Ion Jet Interaction Generator (HIJING) Monte Carlo model is updated with the latest parton distributions functions and a new set of the parameters in the two-component minijet model that controls the total $p + p$ cross section and the central pseudorapity density. We study hadron spectra and multiplicity distributions using the HIJING 2.0 model and compare to recent experimental data from $p + p$ collisions at the Large Hadron Collider (LHC) energies. We also give predictions of hadron production in $p + p$, $p + \text{Pb}$, and $\text{Pb} + \text{Pb}$ collisions at the full LHC energy.

I. INTRODUCTION

The Heavy-Ion Jet Interaction Generator (HIJING) Monte Carlo model was developed to study hadron production in high-energy nucleon-nucleon, nucleon-nucleus, and nucleus-nucleus collisions [1–3]. It was based on a two-component geometrical model of minijet production and soft interaction and has incorporated nuclear effects such as nuclear modification of the parton distribution functions and jet quenching via final-state jet medium interaction. It can reproduce most features of hadron production in $p + p(\bar{p})$ and $p + A$ collisions up to the Fermilab Tevatron energies. With some modification of the string configuration in the soft sector of particle production, it can also reproduce the bulk hadron spectra and can approximate the suppression of high p_T hadrons owing to jet quenching in the central rapidity region of $A + A$ collisions up to the Relativistic Heavy Ion Collider (RHIC) energies [4–6]. It has been widely used to simulate hadron production in $p + A$ and $A + A$ collisions for designs of new detector systems and provide initial conditions for parton and hadron cascade models such A Multiphase Transport (A Multi-Phase Transport) model [7].

The core component of HIJING is the two-component model for beam parton interaction, which was proposed to model the energy dependence of total cross section [8–14] and particle production [15–18] in high-energy hadron collisions. The two-component model was also extended [19,20] and later incorporated in the HIJING model to describe initial parton production in high-energy, heavy-ion collisions. In this two-component model, one assumes that parton interaction in high-energy nucleon-nucleon collisions can be divided into soft interaction and hard or semihard interaction with jet production. A cutoff scale p_0 in the transverse momentum of the final jet production has to be introduced below which the interaction is considered nonperturbative and can only be characterized by a finite soft parton cross section σ_{soft}. For jet production with a transverse momentum $p_T > p_0$, the cross section and jet spectrum are assumed to be given by a perturbative quantum choromodynamics (QCD) parton model.

Jet cross sections in a collinear factorized perturbative QCD, in turn, depend on the parton distribution functions (PDFs) that are parametrized from a global fit to the available experimental data of deeply inelastic scattering (DIS) of lepton and nucleon, Drell-Yan lepton pair, direct photon, and jet production in $p + p(\bar{p})$ collisions.

The two parameters σ_{soft} and p_0 in HIJING are determined phenomenologically by fitting the experimental data of total cross sections and hadron multiplicity in $p + p/\bar{p}$ collisions, which should depend on the parametrization of nucleon PDFs. In the original version of HIJING, Duke-Own parametrization [21] of PDFs is used to calculate the jet production cross section with $p_T > p_0$, which is adequate for the description of jet production at RHIC and maybe Tevatron energies. However, for $p + p$ collisions at much higher energies such as the LHC energies, jet production processes involve initial beam partons with a fraction momentum $x \sim 10^{-4}$, where Duke-Owen parametrization of PDFs is no longer valid. More modern parametrizations should be used. In this progress report, we introduce the HIJING 2.0 model, in which we use a more modern set of parameterized PDFs. We have to perform a global fit of the total cross sections and hadron multiplicities in $p + p(\bar{p})$ collisions to determine the two parameters, σ_{soft} and p_0, and their energy dependence. We will use the new HIJING 2.0 model to study hadron production in $p + p$ at the LHC energies and compare to recently published experimental data. We also provide predictions of hadron multiplicities in $p + p$ and $\text{Pb} + \text{Pb}$ collisions at the full LHC energies.

II. TWO-COMPONENT MODEL IN HIJING

In the two-component model [1–3,8–14] incorporated in HIJING, one assumes that events of nucleon-nucleon collisions at high energies can be divided into soft and hard processes with at least one pair of jet production with $p_T > p_0$. The inclusive jet cross section σ_{jet} in the leading order (LO) [22],

$$\sigma_{\text{jet}} = \int_{p_0^2}^{s/4} dp_T^2 \, dy_1 \, dy_2 \frac{1}{2} \frac{d\sigma_{\text{jet}}}{dp_T^2 \, dy_1 \, dy_2}, \tag{1}$$

$$\frac{d\sigma_{\mathrm{jet}}}{dp_T^2 \, dy_1 \, dy_2}$$
$$= K \sum_{a,b} x_1 f_a\left(x_1, p_T^2\right) x_2 f_b\left(x_2, p_T^2\right) \frac{d\sigma^{ab}(\hat{s}, \hat{t}, \hat{u})}{d\hat{t}}, \quad (2)$$

depends on the parton-parton cross section σ^{ab} and parton distribution functions $f_a(x, p_T^2)$ in a parametrized form of experimental data of other high-energy DIS and nucleon-nucleon collisions, where the summation runs over all parton species, y_1 and y_2 are the rapidities of the scattered partons, x_1 and x_2 are the light-cone momentum fractions carried by the initial partons, and $K \approx 2$ accounts for the next-to-leading order (NLO) corrections to the LO jet cross section.

Within the eikonal formalism [8–13,23], the nucleon-nucleon cross sections can be expressed in the impact-parameter representation as

$$\sigma_{\mathrm{el}} = \pi \int_0^\infty db^2 \left[1 - e^{\chi(b,s)}\right]^2, \quad (3)$$

$$\sigma_{\mathrm{in}} = \pi \int_0^\infty db^2 \left[1 - e^{2\chi(b,s)}\right], \quad (4)$$

$$\sigma_{\mathrm{tot}} = 2\pi \int_0^\infty db^2 \left[1 - e^{\chi(b,s)}\right], \quad (5)$$

in the limit where the real part of the parton-parton scattering amplitude can be neglected. The eikonal functions $\chi(b, s)$ at an impact parameter b are therefore real and can be expressed in terms of an inclusive jet cross section in perturbative QCD (pQCD) and an effective cross section for the nonperturbative soft parton-parton collisions within the two-component model [1],

$$\chi(b, s) \equiv \chi_s(b, s) + \chi_h(b, s)$$
$$= \tfrac{1}{2}[\sigma_{\mathrm{soft}} T_{NN}(b) + \sigma_{\mathrm{jet}} T_{NN}(b)], \quad (6)$$

where $T_{NN}(b)$ is the nucleon-nucleon overlap function and will be assumed to take the form of the Fourier transformation of a dipole form factor in HIJING.

Within the above eikonal implementation of the two-component model, one can also calculate the nucleon-nucleon cross section [18] for no jet and $j \geqslant 1$ number of jet production with $p_T > p_0$,

$$\sigma_0 = \pi \int_0^\infty db^2 \left[1 - e^{-2\chi_s(b,s)}\right] e^{-2\chi_h(b,s)}, \quad (7)$$

$$\sigma_j = \pi \int_0^\infty db^2 \frac{[2\chi_h(b, s)]^j}{j!} e^{-2\chi_h(b,s)}. \quad (8)$$

Their sum gives rise to the total inelastic cross section in Eq. (4). The above eikonal formalism is the basis for the Monte Carlo simulation of multiple jet production in $p + p$, $p + A$, and $A + A$ collisions. Both σ_{soft} and the transverse momentum cutoff p_0 are considered parameters in the HIJING model and are fits to the total and inelastic nucleon-nucleon cross sections and the hadron multiplicity density in the middle rapidity $y = 0$ at each colliding energy.

One can find a detailed description of the HIJING model for hadron production in $p + p$, $p + A$, and $A + A$ collisions in Ref. [1]. The main features of HIJING are as follows:

(i) Multiple minijet production are simulated according to the above eikonal formalism for each nucleon-nucleon collision at a given impact parameter b. The kinematics of each pair of jets and the associated initial and final-state radiation are simulated by using the PYTHIA model [16].

(ii) Events without jet production (with $p_T > p_0$) and the underlying soft parton interaction in events with jet production are modeled by excitation of quark-diquark strings with gluon kinks along the lines of the FRITIOF model [24] and the DPM model [14,25]. In addition, multiple low-p_T exchanges among the end-point constituents are included.

(iii) A set of impact-parameter-dependent parton distribution functions is used to include nuclear modification of the parton distribution functions inside the nuclei.

(iv) A simple model for jet quenching is used to study the effect of jet medium interaction in $A + A$ collisions [26].

III. UPDATES IN HIJING

In the default setting of HIJING 1.0 [1], Duke-Owens parametrization [21] of PDFs in nucleons is used. With Duke-Owens parametrization of PDFs, an energy-independent cutoff scale $p_0 = 2$ GeV/c and a constant soft parton cross section $\sigma_{\mathrm{soft}} = 57$ mb are sufficient to reproduce the experimental data on total and inelastic cross sections and the hadron central rapidity density in $p + p/\bar{p}$ collisions [27]. Duke-Owens parametrization of PDFs is known to be very outdated, and one needs to use more modern parametrizations from new global fits to experimental data, especially at the LHC energies when minijet production reaches to a very small-x region of the parton distribution, where gluon distribution is much higher than Duke-Owens parametrization.

Furthermore, with a constant transverse momentum cutoff $p_0 = 2$ GeV/c in HIJING 1.0, the total number of minijets per unit transverse area could exceed the limit

$$\frac{T_{AA}(b) \, \sigma_{\mathrm{jet}}}{\pi R_A^2} \leqslant \frac{p_0^2}{\pi} \quad (9)$$

for independent multiple jet production even in central $p + p$ collisions for sufficiently large inclusive jet cross sections at high colliding energies, where $T_{AA}(b)$ is the overlap function of $A + A$ collisions and π/p_0^2 is the intrinsic transverse size of a minijet with transverse momentum p_0. Therefore, one inevitably has to increase the value of the transverse momentum cutoff p_0 to ensure the applicability of the underlying two-component model of independent multiple jet production in the HIJING model.

In the updated version of HIJING 2.0, we will use the Gluck-Reya-Vogt (GRV) parametrization [28] of PDFs, among many modern parametrizations of the PDFs that are available. The gluon distributions in this new parametrization are much higher than the old Duke-Owens parametrization at small x, and therefore give much larger inclusive jet cross sections at high colliding energies with a fixed value of cutoff p_0. One therefore can no longer fit the experimental $p + p/\bar{p}$ data on

total and inelastic cross sections by using a constant cutoff p_0 and the soft parton cross section σ_{soft} within the two-component model. One has to assume an energy-dependent cutoff $p_0(\sqrt{s})$ and soft cross section $\sigma_{soft}(\sqrt{s})$ [29]. Fitting the experimental values of the total and inelastic cross sections of $p + p/(\bar{p})$ collisions, including those extracted from cosmic experimental and hadron central rapidity density, we have the following parametrized energy dependence of the cutoff and the soft parton cross section used in the two-component model of HIJING 2.0:

$$p_0 = 2.62 - 1.084 \log(\sqrt{s}) + 0.299 \log^2(\sqrt{s}) - 0.0292 \log^3(\sqrt{s}) + 0.00151\log^4(\sqrt{s}), \quad (10)$$

$$\sigma_{soft} = 55.316 - 4.1126 \log(\sqrt{s}) + 0.854 \log^2(\sqrt{s}) - 0.0307 \log^3(\sqrt{s}) + 0.00328 \log^4(\sqrt{s}), \quad (11)$$

where the colliding energy $\sqrt{s}$ in center-of-mass frame is in units of GeV. Shown in Fig. 1 are the calculated
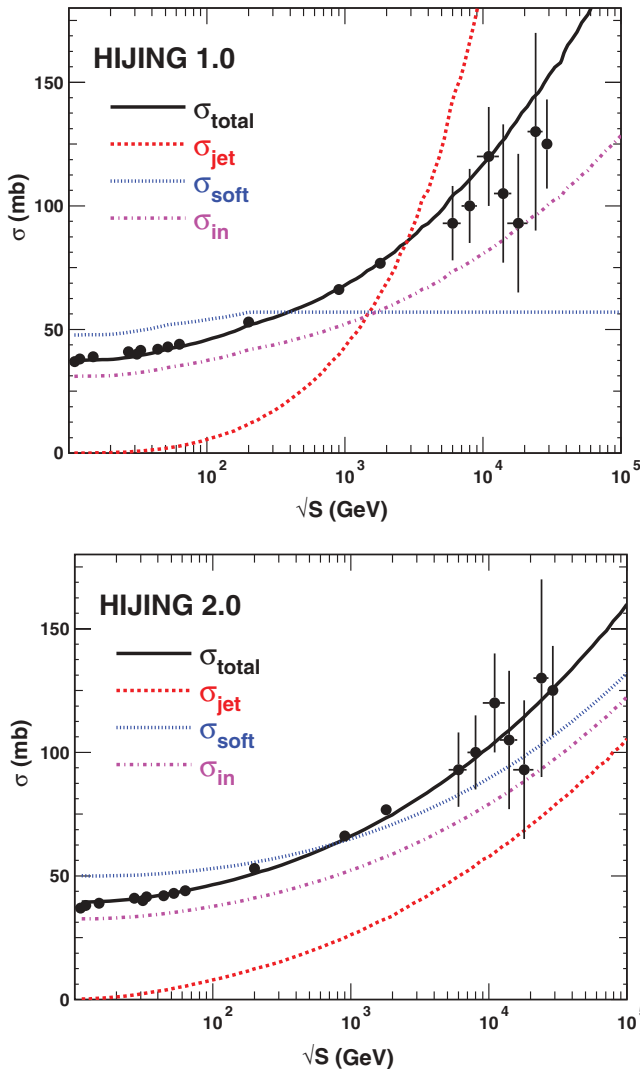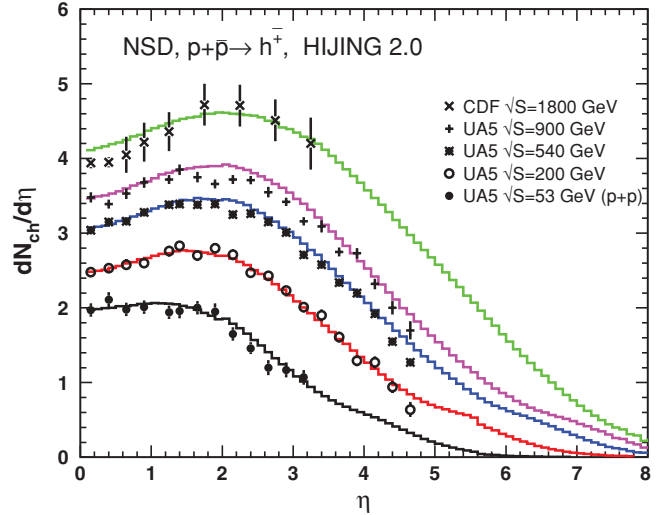

FIG. 2. (Color online) Pseudorapidity distributions of charged particles in NSD pp at $\sqrt{s} = 53$ GeV, $p\bar{p}$ collisions at $\sqrt{s} = 200$, 540, 900, and 1800 GeV as compared to experimental data [37,38].

total and inelastic cross sections using both HIJING 1.0 and HIJING 2.0 as compared to the experimental data. The total inclusive jet cross section and nonperturbative soft parton cross sections are also plotted for illustration. With a constant cutoff $p_0 = 2$ GeV/c and soft parton cross section σ_{soft} at high colliding energies, HIJING 1.0 already gives a larger total cross section than the cosmic data indicate even with the Duke-Owens parametrization of PDFs. With much higher gluon distribution at small x in the GRV parametrization used in HIJING 2.0, one has to introduce a cutoff p_0 and the soft parton cross section σ_{soft} that increases with colliding energy in order to fit the experimental data on the total cross section. There are, however, some freedom in fixing the values of p_0 and σ_{soft}, which is further constrained by the energy dependence of the central rapidity density of the charged multiplicities, as shown in Fig. 2. The increasing cutoff as required by the experimental data indicates that multiple minijet production below such a cutoff is no longer independent and coherent interaction becomes important. This might be taken as an indirect evidence of gluon saturation at very small x inside a proton in proton-proton collisions at very high energies, especially at the LHC energies. An alternative approach to effectively take into account such gluon saturation is to increase the string tension of soft hadron production as proposed in Ref. [30]. We choose to focus on the change of minijet production in HIJING 2.0.

We also show in Fig. 3 the transverse momentum spectra calculated with HIJING 2.0 at different colliding energies as compared to the experimental data. HIJING 2.0 results are all in good agreement with the experimental data.

Note that both HIJING 2.0 calculations and data shown in Fig. 2 are for non-single-diffractive (NSD) events. The definitions of NSD triggers are different in different experiments, leading to different central pseudorapidity densities in these NSD events. The NSD triggers in the UA5 experiment require at least one charged particle simultaneously in each of the pseudorapidity regions at both ends covering $2 < |\eta| < 5.6$,
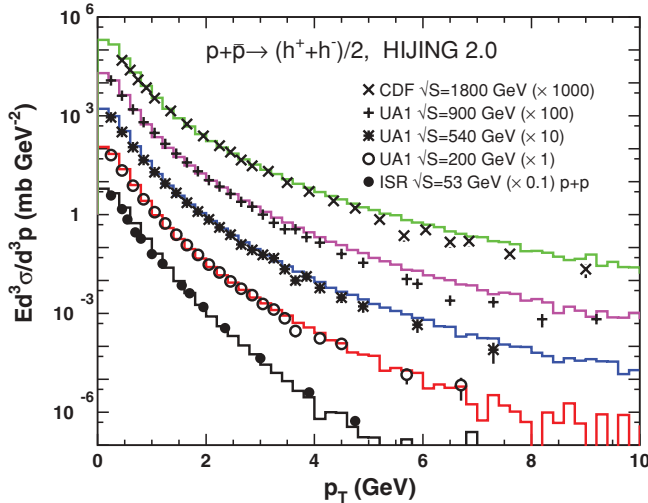

FIG. 1. (Color online) Total, soft, and jet production cross sections of pp and $p\bar{p}$ collisions. The histograms in the the upper panel are calculated using HIJING 1.0, while the lower histograms are calculated using HIJING 2.0. The data are from Refs. [31–36].

FIG. 3. (Color online) Invariant inclusive cross sections of charged particles in pp at $\sqrt{s} = 53$ GeV, $p\bar{p}$ collisions at $\sqrt{s} = 200$, 500, 900, and 1800 GeV. The data come from Refs. [39–41]. Both the calculation and experimental data are obtained in the region of $|\eta| < 2.5$ for $\sqrt{s} = 200$, 540, and 900 GeV, and $|\eta| < 1.0$ for $\sqrt{s} = 53$ and 1800 GeV.

while Collider-Detector at Fermilab (CDF) NSD events are triggered in $3.2 < |\eta| < 5.9$. The increase of the central pseudorapidity density with energy can be attributed to the increased minijet production in high colliding energies.

IV. HADRON SPECTRA IN $p + p$ AND $A + A$ COLLISIONS AT THE LHC ENERGIES

With the updated HIJING 2.0, we can study hadron production in $p + p$ and $A + A$ collisions at the LHC energies. At the highest energy of $\sqrt{s} = 14$ TeV, minijet production involves partons in the very small x region. The increase of the cutoff for independent minijet production required to fit the total cross section can be considered as an indication of coherence or gluon saturation inside protons at very high energies. This will certainly affect the produced hadron pseudorapidity distribution at the LHC energies. Shown in Fig. 4 is the energy dependence of the central pseudorapidity density of charged hadrons $dN_{ch}/d\eta$ averaged over $|\eta| < 1.0$ as a function of the colliding energy in inelastic $p + p$ collisions from both HIJING 1.0 and HIJING 2.0 calculations as compared to experimental data, including that measured in $p + p$ collisions at $\sqrt{s} = 0.9$ and 2.36 TeV from A Large Ion Collider Experiment (ALICE) [45] at the LHC. The central rapidity hadron density in HIJING 2.0 continues to increase with the colliding energy at LHC more or less in a double logarithm form. Because of the larger values of cutoff for minijet production, the central rapidity hadron density in HIJING 2.0 is significantly lower than HIJING 1.0 at the LHC energies.

Shown in Figs. 5 and 6 are HIJING results for the pseudorapidity distributions of charged hadrons in $p + p$ at $\sqrt{s} = 0.9$, 2.36, and 7 TeV in inelastic and NSD events. The central rapidity density in NSD events is generally larger than in inelastic events, and HIJING results agree reasonably well with
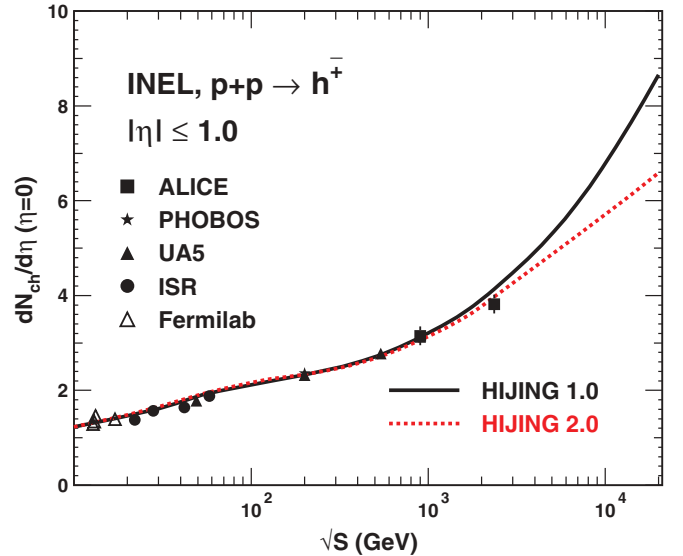
the experimental data. Note that the Compact Muon Solenoid (CMS) [46,47] experiment uses a different definition of NSD events that gives slightly higher averaged multiplicity than that with UA5 definition of NSD events in HIJING calculations. Another class of inelastic events in ALICE experiments (INEL > 0) is defined by requiring at least one charged tracks within $|\eta| < 1$. HIJING results for these type of events (short-dashed lines) are similar to the inelastic events because the lack of double-diffractive events in the Monte Carlo model. Both single diffractive and non-diffractive events in HIJING have a finite value of multiplicity in the central rapidity region. This disagrees with the ALICE data [45], which are
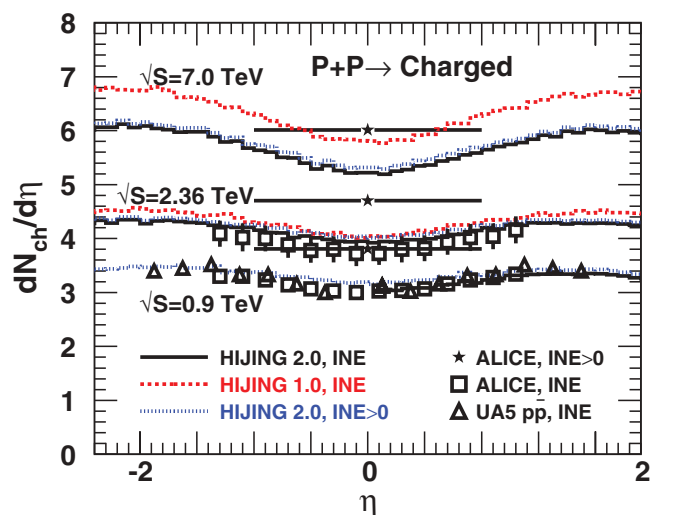

FIG. 4. (Color online) Central pseudorapidity density at $\eta = 0$ for charged particles produced in $p + p/\bar{p}$ collisions as a function of $\sqrt{s}$. The experimental data are from Refs. [37,42–45].

FIG. 5. (Color online) Pseudorapidity distribution $dN_{ch}/d\eta$ in inelastic $p + p$ collisions at LHC energies. The experiment data are from UA5 [37], ALICE [45], and CMS [46,47]. Shown as the short-dashed lines are the HIJING results for ALICE-defined INEL > 0 events in which at least one charged track is required within $|\eta| < 1$.
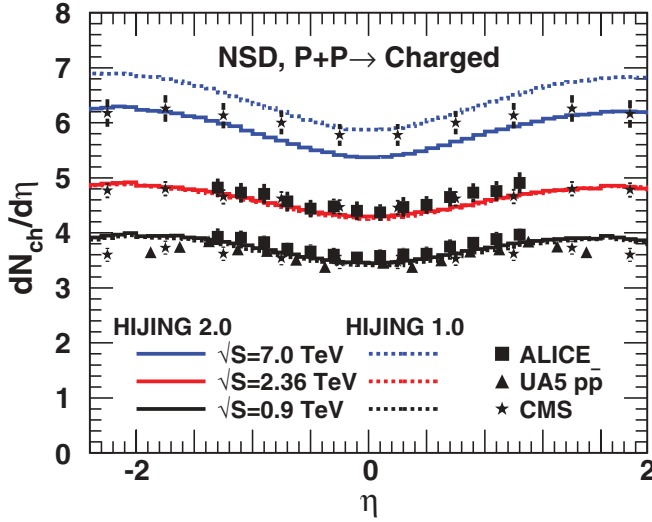
FIG. 6. (Color online) Pseudorapidity distribution $dN_{ch}/d\eta$ in NSD $p + p$ collisions at LHC energies. The experiment data are from UA5 [37], ALICE [45], and CMS [46,47]. The definitions of NSD events in our calculations and the experimental data from ALICE and UA5 follow that in the UA5 experiment, as described in the text. CMS [46,47] uses a different definition .

even larger than the central rapidity density in NSD events. Such a discrepancy in the trigger dependence of the averaged multiplicity can be fixed when double-diffractive events are included in future improvements of HIJING. However, this is not expected to have a significant influence on particle production in heavy-ion collisions because the fraction of diffractive interactions becomes increasingly smaller in multiple nucleon-nucleon collisions.

Shown in Figs. 7 and 8 are the multiplicity distributions for charged hadrons within a different pseudorapidity range in inelastic and NSD $p + p$ collisions at the LHC energies from HIJING calculations as compared to experimental data from the ALICE experiment [45]. HIJING results agree reasonably well with the data in low and intermediate multiplicities. However, they fall short of the experimental data at higher multiplicity
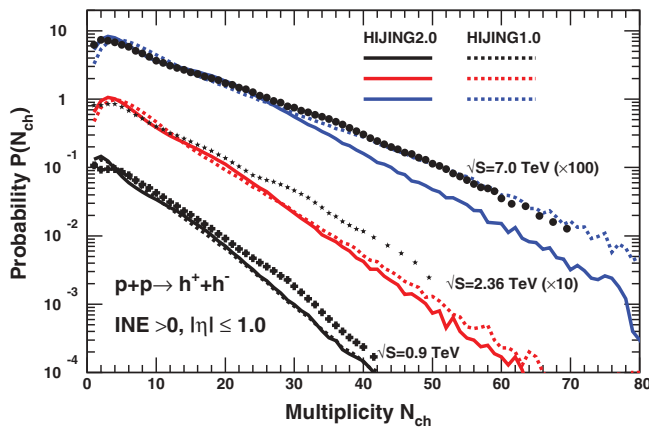

FIG. 7. (Color online) Multiplicity distributions for changed hadrons within $|\eta| < 1$ in inelastic $p + p$ collisions at LHC energies from the ALICE [45] experiment compared to HIJING results.
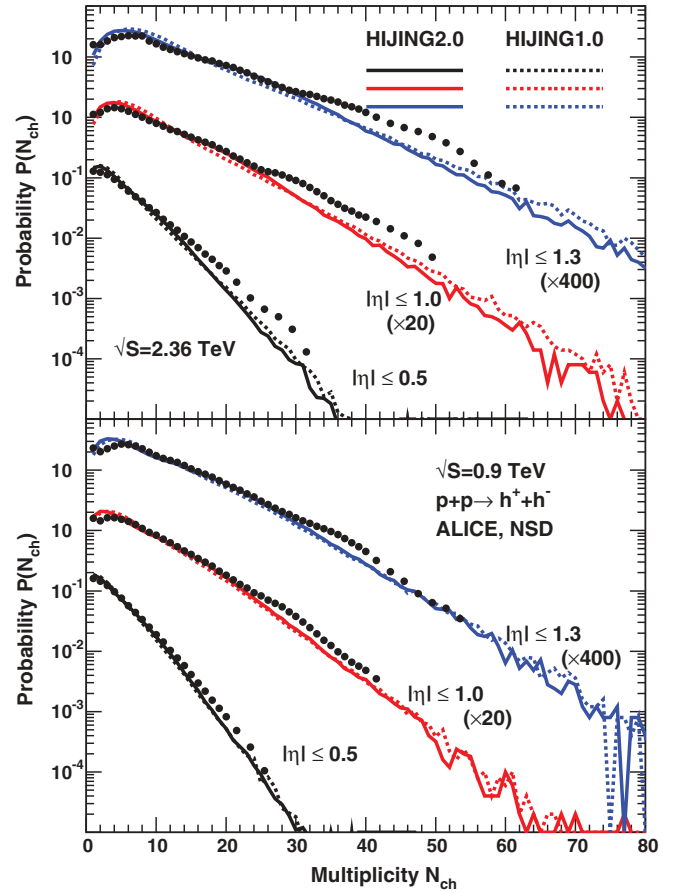

FIG. 8. (Color online) Multiplicity distributions for charged hadrons within different pseudorapidity intervals in NSD events of $p + p$ collisions at $\sqrt{s} = 2.36$ TeV from the ALICE [45] experiment as compared to HIJING results.

tails, in particular at $\sqrt{s} = 7$ TeV. These high multiplicity events are dominated by multiple jets and they are likely to have final-state interactions with each other, as indicated by the ridge structure in the two-hadron correlation in the azimuthal angle and the large rapidity gap observed in the CMS experiment [48]. The final-state interaction in these high multiplicity events could affect the multiplicity distribution, which is not included in the current HIJING model.

At high colliding energies, the transverse momentum of produced hadrons should be dominated by hadrons from jet fragmentation, especially at a large transverse momentum, as shown in Fig. 9. We compare the HIJING 2.0 results to the ALICE [49] experimental data on charged hadrons within $|\eta| < 0.8$ in inelastic $p + p$ collisions at $\sqrt{s} = 0.9$ TeV, and CMS [46,47] data on charged hadrons within $|\eta| < 2.4$ in NSD $p + p$ collisions at $\sqrt{s} = 0.9$, 2.36, and 7 TeV. The HIJING 2.0 results at $\sqrt{s} = 14$ TeV for inelastic events in $p + p$ collisions are also shown. Within the LHC energy range $\sqrt{s} = 0.9$–14 TeV, the transverse momentum spectra at a large p_T region becomes apparently harder at higher colliding energies. Even though the cutoff for minijet production in HIJING 2.0 is significantly larger than in HIJING 1.0, hadronization from partons as results of initial and final-state radiation still fills in the hadron transverse
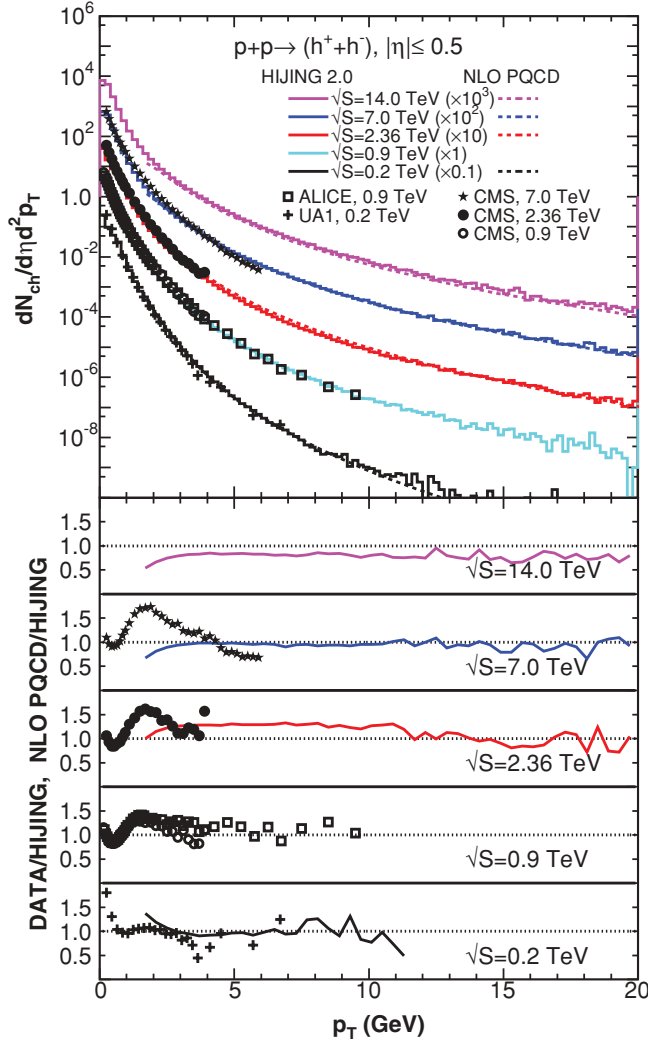
FIG. 9. (Color online) Transverse momentum distributions of charged hadron in $p + p$ collisions. The experimental data are from ALICE [49] (open squares) for inelastic $p + p$ collisions and CMS [46] (open and closed circles) for NSD $p + p$ collisions at $\sqrt{s} = 0.9$ and 2.36 TeV. The histograms are results from HIJING 2.0.

momentum spectra in the intermediate transverse momentum. HIJING 2.0 describes reasonably well the ALICE and CMS experimental data at the LHC energies with a maximum discrepancy of 50% at small $p_T \sim 2$ GeV, as shown in the lower panels in Fig. 9, where the ratios of data over HIJING results are plotted. The transverse momentum spectra in this small p_T region also can be influenced by final-state interaction among jets. We also plot the ratios of charged hadron spectra from NLO pQCD calculations [50,51] over Those from HIJING. HIJING reproduces the NLO pQCD results very well over a large p_T range and at different colliding energies.

To describe hadron production in $A + A$ collisions, one should include both the nuclear modification of the parton distribution functions and jet quenching in the final-state interaction. Jet quenching, in general, suppresses high transverse momentum hadrons [26]. Because the yields of these high transverse momentum partons are relatively small as compared to the bulk part of the initial parton production, its effect

on the total hadron multiplicity in $A + A$ collisions will be small as illustrated by other model studies [52–55] of hadron production in heavy-ion collisions at RHIC, most of which have also neglected the effect of final-state interaction. With two parameters (p_0 and σ_{soft}) fixed from fit to $p + p$ collisions, the only uncertainty for hadron multiplicity density in $A + A$ collisions is the nuclear modification of parton distribution functions—gluon distributions in particular—at small x. We assume that parton distributions in nuclei,

$$f_a^A(x, Q^2) = A R_a^A(x, Q^2) f_a^N(x, Q^2), \qquad (12)$$

are given by that in the nucleon and the modification factor $R_a^A(x, Q^2)$. This nuclear modification has been studied with data from DIS and Drell-Yan lepton pair production experiments. However, most of the parametrizations [56,57] do not have gluon shadowing strong enough to give the central multiplicity density as measured in RHIC experiments within the two-component model as implemented in the HIJING model. We will use the new HIJING parametrization [29], which introduced a strong impact-parameter dependence of the parton shadowing in order to fit the centrality dependence of the central multiplicity density at RHIC. The shadowing factors for quarks and gluons are

$$R_q^A(x, b) = 1.0 + 1.19 \log^{1/6} A(x^3 - 1.2x^2 + 0.21x)$$
$$- s_q(b)(A^{1/3} - 1)^{0.6}(1 - 3.5\sqrt{x})$$
$$\times \exp(-x^2/0.01), \qquad (13)$$
$$R_g^A(x, b) = 1.0 + 1.19 \log^{1/6} A(x^3 - 1.2x^2 + 0.21x)$$
$$- s_g(b)(A^{1/3} - 1)^{0.6}(1 - 1.5x^{0.35})$$
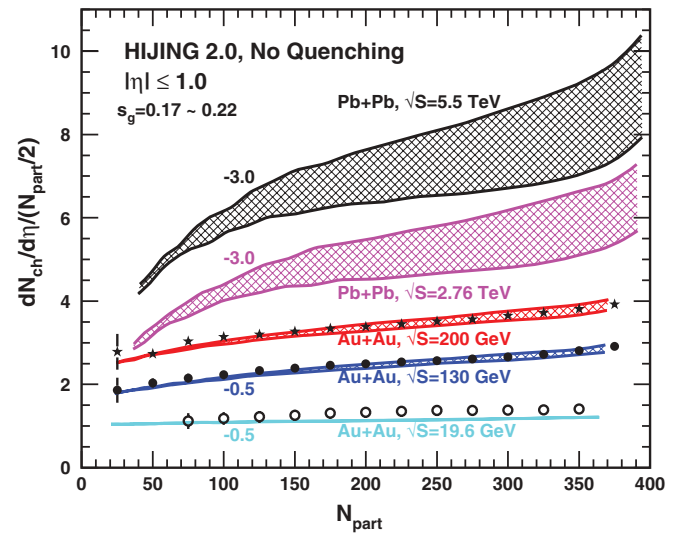$$\times \exp(-x^2/0.004), \qquad (14)$$

FIG. 10. (Color online) Pseudorapidity density per participant pair as a function of the average number of participants in heavy-ion collisions at different energies from HIJING 2.0 calculations. Dashed lines are HIJING 1.0 results. The experimental data are from Ref. [59]. Note that a vertical ofset is applied to each curve for clear illustration.

respectively. The impact-parameter dependence of the shadowing is implemented through the parameters

$$s_a(b) = s_a \frac{5}{3}\left(1 - b^2/R_A^2\right),　　　　(15)$$

where $R_A = 1.12A^{1/3}$ is the nuclear size. The value $s_q = 0.1$ is fixed by the experimental data on DIS off nuclear targets [29], and $s_g = 0.17$–0.22 is chosen to fit the RHIC experimental by using the HIJING 2.0 model as shown in Fig. 10. The form of the impact parameter dependence is chosen to give rise to the centrality dependence of the pseudorapidity multiplicity density per participant pair, and the range of values of s_g is allowed by experimental errors at the RHIC energies. With this parametrization of parton shadowing, one can calculate the pesudorapidity multiplicity density per participant pair in Pb + Pb collisions at the LHC energies as a function of the number of participants shown in Fig. 10. As a comparison, we also show results from HIJING 1.0 as dashed lines in Fig. 10. The range of the gluon shadowing parameter s_g allowed at RHIC leads to much bigger uncertainties in the multiplicity density at the LHC energies. With such strong gluon shadowing constrained by the RHIC data, the effective minijet cross section at the LHC energies is still much larger than at RHIC, and
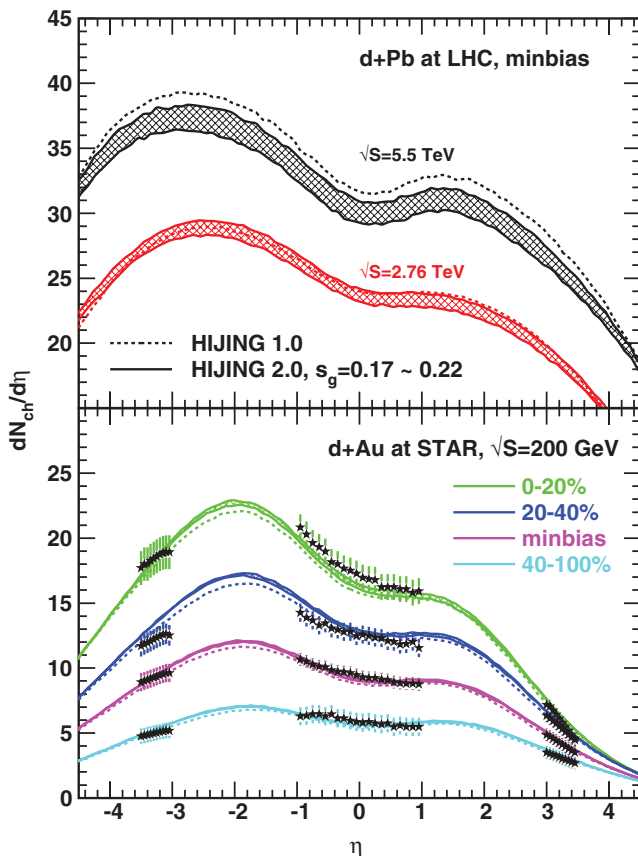

FIG. 11. (Color online) Pseudorapidity distributions of charged hadrons in $d + $ Au collisions at the RHIC energy $\sqrt{s} = 200$ GeV/n (lower panel) and $d + $ Pb collisions (upper panel) at the LHC energies. The solid lines are HIJING 2.0 results with the bands corresponding to the variation of the gluon nuclear shadowing parameter $s_g = 0.19$–0.24. Data at the RHIC energy are from the STAR experiment [60].

therefore the minijet component leads to a stronger centrality (N_{part}) dependence of the central pseudorapidity density of produced hadrons. This strong centrality dependence is very different from other model predictions [58], such as the color glass condensate (CGC) or the limiting fragmentation model. Therefore, the first experimental data on the hadron production at LHC will shed light on the parton and hadron production mechanism in high-energy hadron and nuclear collisions.

To constrain parton shadowing in the nucleus, one, in principle, can also study hadron production in $d + A$ collisions. Shown in the lower panel of Fig. 11 are the pseudorapidity distributions of charged hadrons in $d + $ Au collisions at the RHIC energy $\sqrt{\,} = 200$ GeV for different centralities and minimum-bias events as compared to the Solenoidal Tracker At RHIC (STAR) data [60]. Within the experimental errors, both HIJING 2.0 (solid bands) and HIJING 1.0 can describe the data reasonably well. We have followed the definition for the selection of centrality in the STAR measurements. The solid bands in the HIJING 2.0 calculation as a variation of the gluon shadowing parameter s_g constrained by RHIC data of Au + Au collisions are too small to be discerned by the $d + $ Au data. A similar situation occurs in $d + $ Pb collisions at the LHC energy, as shown in the upper panel of Fig. 11. The change of the pesudorapidity distribution owing to a variation of the gluon nuclear shadowing parameter is much smaller than in central Pb + Pb collisions shown in Fig. 10. The difference between HIJING 2.0 and HIJING 1.0 in $d + $ Pb collisions becomes significant only at the highest energy $\sqrt{s} = 5.5$ TeV, reflecting the $p + p$ results in Fig. 4.

V. CONCLUSIONS

We have updated the HIJING Monte Carlo model with modern parton distribution functions for nucleons and a new set of parameters within the two-component model for minijet production in high-energy nucleon-nucleon collisions. Because of the large gluon distribution at small x in the GRV [28], parametrization of the nucleon's PDFs used in HIJING 2.0, one has to introduce an energy-dependent transverse momentum cutoff p_0 for the minijet production and the soft parton interaction cross section σ_{soft} in order to describe the energy dependence of the total inelastic cross sections and the central rapidity hadron density in high-energy $p + p(\bar{p})$ collisions. The updated HIJING 2.0 model is shown to describe the existing experimental data on hadron production from Intersecting Storage Rings (ISR) energy up to the Fermilab Tevatron energy. The HIJING 2.0 results are also shown to be in good agreement with the recently published hadron spectra in $p + p$ collisions at the LHC energies ($\sqrt{s} = 0.9$ and 2.36 TeV), except for events with INEL > 0 trigger because of the lack of double-diffractive events in the model of soft interaction in HIJING. We also give the HIJING 2.0 predictions for $p + p$ collisions at $\sqrt{s} = 7$ and 14 TeV. With a model parametrization for nuclear modification of the parton distribution functions, we also give a HIJING 2.0 prediction of hadron multiplicity in central Pb + Pb and minimum-bias events of $d + $ Pb collisions at the LHC energies $\sqrt{s} = 2.75$ and 5.5 TeV/n.

This is the first step in the upgrade to the HIJING model. The Jet quenching description in the current HIJING model is very schematic. The next stage in the upgrade of HIJING will be focused on jet quenching in a dense medium, incorporating the most recent developments [61–65] in the theory of parton propagation and multiple interaction in a dense medium.

ACKNOWLEDGMENTS

[1] X. N. Wang and M. Gyulassy, Phys. Rev. D **44**, 3501 (1991).

[2] M. Gyulassy and X. N. Wang, Comput. Phys. Commun. **83**, 307 (1994).

[3] X. N. Wang, Phys. Rep. **280**, 287 (1997).

[4] S. E. Vance, M. Gyulassy, and X. N. Wang, Phys. Lett. B **443**, 45 (1998).

[5] S. E. Vance and M. Gyulassy, Phys. Rev. Lett. **83**, 1735 (1999).

[6] V. T. Pop, M. Gyulassy, J. Barrette, C. Gale, X. N. Wang, and N. Xu, Phys. Rev. C **70**, 064906 (2004).

[7] B. Zhang, C. M. Ko, B. A. Li, and Z. Lin, Phys. Rev. C **61**, 067901 (2000).

[8] T. K. Gaisser and F. Halzen, Phys. Rev. Lett. **54**, 1754 (1985).

[9] P. L'Heureux, B. Margolis, and P. Valin, Phys. Rev. D **32**, 1681 (1985).

[10] G. Pancheri and Y. N. Srivastava, Phys. Lett. B **182**, 199 (1986).

[11] L. Durand and H. Pi, Phys. Rev. Lett. **58**, 303 (1987); Phys. Rev. D **38**, 78 (1988).

[12] J. Dias de Deus and J. Kwiecinski, Phys. Lett. B **196**, 537 (1987).

[13] R. C. Hwa, Phys. Rev. D **37**, 1830 (1988).

[14] A. Capella, U. Sukhatme, and J. Tran Thanh Van, Z. Phys. C **3**, 329 (1979).

[15] T. K. Gaisser, F. Halzen, and A. D. Martin, Phys. Lett. B **166**, 219 (1986).

[16] T. Sjostrand and M. van Zijl, Phys. Rev. D **36**, 2019 (1987); T. Sjostrand, Comput. Phys. Commun. **39**, 347 (1986).

[17] W. R. Chen and R. C. Hwa, Phys. Rev. D **39**, 179 (1989).

[18] X. N. Wang, Phys. Rev. D **43**, 104 (1991).

[19] J. P. Blaizot and A. H. Mueller, Nucl. Phys. B **289**, 847 (1987).

[20] K. Kajantie, P. V. Landshoff, and J. Lindfors, Phys. Rev. Lett. **59**, 2527 (1987); K. J. Eskola, K. Kajantie, and J. Lindfors, Nucl. Phys. B **323**, 37 (1989).

[21] D. W. Duke and J. F. Owens, Phys. Rev. D **30**, 49 (1984).

[22] E. Eichten, I. Hinchliffe, K. D. Lane, and C. Quigg, Rev. Mod. Phys. **56**, 579 (1984); **58**, 1065 (1986).

[23] A. Capella and J. Tran Thanh Van, Z. Phys. C **23**, 165 (1984); **25**, 102(E) (1984).

[24] B. Andersson, G. Gustafson, and B. Nilsson-Almqvist, Nucl. Phys. B **281**, 289 (1987); B. Nilsson-Almqvist and E. Stenlund, Comput. Phys. Commun. **43**, 387 (1987).

[25] J. Ranft, Phys. Rev. D **37**, 1842 (1988); Phys. Lett. B **188**, 379 (1987).

[26] X. N. Wang and M. Gyulassy, Phys. Rev. Lett. **68**, 1480 (1992).

[27] X. N. Wang and M. Gyulassy, Phys. Rev. D **45**, 844 (1992).

[28] M. Gluck, E. Reya, and A. Vogt, Z. Phys. C **67**, 433 (1995).

[29] S. Y. Li and X. N. Wang, Phys. Lett. B **527**, 85 (2002).

[30] V. Topor Pop, M. Gyulassy, J. Barrette, C. Gale, S. Jeon, and R. Bellwied, Phys. Rev. C **75**, 014904 (2007).

[31] U. Amaldi and K. R. Schubert, Nucl. Phys. B **166**, 301 (1980).

[32] M. Bozzo et al. (UA4 Collaboration), Phys. Lett. B **147**, 392 (1984).

[33] G. J. Alner et al. (UA5 Collaboration), Z. Phys. C **32**, 153 (1986).

[34] N. A. Amos et al. (E710 Collaboration), Phys. Rev. Lett. **63**, 2784 (1989).

[35] R. M. Baltrusaitis et al., Phys. Rev. Lett. **52**, 1380 (1984).

[36] T. Hara et al., Phys. Rev. Lett. **50**, 2058 (1983); L. Durand and H. Pi, ibid. **58**, 303 (1987).

[37] G. J. Alner et al. (UA5 Collaboration), Z. Phys. C **33**, 1 (1986).

[38] F. Abe et al. (CDF Collaboration), Phys. Rev. D **41**, 2330 (1990).

[39] B. Alper et al. (British-Scandinavian Collaboration), Nucl. Phys. B **87**, 19 (1975).

[40] C. Albajar et al. (UA1 Collaboration), Nucl. Phys. B **335**, 261 (1990).

[41] F. Abe et al. (CDF Collaboration), Phys. Rev. Lett. **61**, 1819 (1988).

[42] W. Thome et al. (Aachen-CERN-Heidelberg-Munich Collaboration), Nucl. Phys. B **129**, 365 (1977).

[43] J. Whitmore, Phys. Rep. **10**, 273 (1974); W. M. Morse et al., Phys. Rev. D **15**, 66 (1977); C. P. Ward et al., Nucl. Phys. B **153**, 299 (1979).

[44] R. Nouicer et al. (PHOBOS Collaboration), J. Phys. G **30**, S1133 (2004).

[45] K. Aamodt et al. (ALICE Collaboration), Eur. Phys. J. C **65**, 111 (2010); **68**, 345 (2010).

[46] V. Khachatryan et al. (CMS Collaboration), J. High Energy Phys. 02 (2010) 041.

[47] V. Khachatryan et al. (CMS Collaboration), Phys. Rev. Lett. **105**, 022002 (2010).

[48] V. Khachatryan et al. (CMS Collaboration), J. High Energy Phys. 09 (2010) 091.

[49] K. Aamodt et al. (ALICE Collaboration), Phys. Lett. B **693**, 53 (2010).

[50] B. W. Harris and J. F. Owens, Phys. Rev. D **65**, 094032 (2002).

[51] H. Zhang, J. F. Owens, E. Wang, and X. N. Wang, Phys. Rev. Lett. **98**, 212301 (2007).

[52] X. N. Wang and M. Gyulassy, Phys. Rev. Lett. **86**, 3496 (2001).

[53] K. J. Eskola, K. Kajantie, and K. Tuominen, Phys. Lett. B **497**, 39 (2001).

[54] Z. W. Lin, S. Pal, C. M. Ko, B. A. Li, and B. Zhang, Phys. Rev. C **64**, 011902 (2001).

[55] D. Kharzeev and M. Nardi, Phys. Lett. B **507**, 121 (2001).
[56] K. J. Eskola, V. J. Kolhinen, and C. A. Salgado, Eur. Phys. J. C **9**, 61 (1999).
[57] M. Hirai, S. Kumano, and M. Miyama, Phys. Rev. D **64**, 034003 (2001).
[58] N. Armesto *et al.*, J. Phys. G **35**, 054001 (2008).
[59] S. S. Adler *et al.* (PHENIX Collaboration), Phys. Rev. C **71**, 034908 (2005); **71**, 049901(E) (2005).
[60] B. I. Abelev *et al.* (STAR Collaboration), Phys. Rev. Lett. **99**, 021603 (2007).
[61] M. Gyulassy and X. N. Wang, Nucl. Phys. B **420**, 583 (1994).
[62] R. Baier, Y. L. Dokshitzer, A. H. Mueller, S. Peigne, and D. Schiff, Nucl. Phys. B **484**, 265 (1997).
[63] U. A. Wiedemann, Nucl. Phys. B **588**, 303 (2000).
[64] M. Gyulassy, P. Levai, and I. Vitev, Nucl. Phys. B **594**, 371 (2001).
[65] X. F. Guo and X. N. Wang, Phys. Rev. Lett. **85**, 3591 (2000); X. N. Wang and X. F. Guo, Nucl. Phys. A **696**, 788 (2001).